Hindawi
Journal of Energy
Volume 2023, Article ID 1842187, 12 pages
https://doi.org/10.1155/2023/1842187

Research Article

Optimization of Syngas Quality for Fischer-Tropsch Synthesis

Ali A. Rabah

Department of Chemical Engineering, University of Khartoum, P.O. Box 321, Khartoum, Sudan

Correspondence should be addressed to Ali A. Rabah; rabahaa1967@gmail.com

Received 30 June 2022; Revised 8 April 2023; Accepted 27 May 2023; Published 19 June 2023

Academic Editor: Kamal Aly

While fossil oil reserves have been receding, the demand for diesel and gasoline has been growing. In recent years, syngas of biomass origin has been emerging as a viable feedstock for Fischer-Tropsch (FT) synthesis, a process for manufacturing synthetic gasoline and diesel. This paper reports the optimization of syngas quality to match the FT synthesis requirement. The optimization model maximizes the thermal efficiency under the constraint of $H_2/CO \geq 2.15$ and operating conditions of equivalent ratio ($ER = 0.0\text{-}1.0$), steam to biomass ratio ($SB = 0.0\text{-}5.0$), and gasification temperature ($T_g = 500^{\circ}\text{C-}1300^{\circ}\text{C}$). The optimization model is executed using the optimization section of the Model Analysis Tools of the Aspen Plus simulator. The model is tested using eleven (11) types of municipal solid waste (MSW). The optimum operating conditions under which the objective function and the constraint are satisfied are $ER = 0$, $SB = 0.66\text{-}1.22$, and $T_g = 679\text{-}763^{\circ}\text{C}$. Under optimal operating conditions, the syngas quality is $H_2 = 52.38\text{-}58.67$ mole percent, lower heating value $(LHV) = 12.55\text{-}17.15$ MJ/kg, and $N_2 = 0.38\text{-}2.33$ mole percent. From an economic point of view, 12.98% to 33.12% of biomass is used as fuel for steam generation, drying, and pyrolysis. The generalized optimization model reported could be extended to any other type of biomass and coal.

1. Introduction

High demand for transportation fuels stems from the growing world population, technological development, and surging transportation volume [1]. In recent years, the quest for feasible substitutes for fossil oil is intensified. Biomass is the most feasible alternative to fossil oil among renewable energy sources for many reasons. Biomass can provide alternative transportation fuels via Fischer-Tropsch (FT) synthesis, a process for the manufacture of synthetic gasoline [2–4]. The world production of biomass is estimated at 146 billion metric tons, equivalent to 52 Gtoe (based on an average higher heating value of 15 MJ/kg). This is more than threefold the world's primary energy demand of 14 Gtoe for the year 2020 [5]. Biomass constituents of C, N, and P can end up in waterways, increasing biochemical oxygen demand (BOD) and causing water pollution. The application of biomass for energy is a recommended solution for waste management [6]. In developing African countries, biomass is negatively priced; the price of biomass of agricultural origin is about USD 60 per ton on a dry basis, relative to the coal price of USD 400 per ton. Bearing in mind that coal's heating value (25-35 MJ/kg) is bout twofold that of biomass (10-20 MJ/kg). Biomass is CO_2 neutral; it absorbs CO_2 in the photosynthesis process to produce glucose as $6CO_2 + 6H_2O \longrightarrow C_6H_{12}O_6 + 6O_2$. In developing countries, biomass abundance and poverty coincide. Therefore, biomass utilization provides income and jobs and initiates socioeconomic development in poor nations. Biomass accounts for 35% of primary energy consumption in developing countries [7].

In light of the above, research on biomass gasification is a high priority. The challenge is to produce syngas with a quality that meets the FT synthesis requirement yet at a high gasification efficiency. This is the objective of this work.

There has been a large volume of research on biomass gasification. Most of the existing research is on the influence of operating conditions and the type of biomass on syngas quality. The operating conditions are equivalence ratio (ER), steam to biomass ratio (SB), and gasification temperature (T_g). Recently, Rabah [8] studied the gasification of ten agricultural residues (bagasse, cotton stalks, sesame straw, groundnut shells, maize straw, sorghum straw, millet straw, sunflower husks, wheat straw, and banana leaves). Begum et al. [9] and Begum et al. [10] studied the gasification of

coffee bean husks, green wastes, food wastes, MSW, pine sawdust, wood chip, and wood residue. Hlavsova et al. [11] studied nine composts obtained from nonhybrid and hybrid perennial grasses. Alex [12] studied prairie cordgrass and switchgrass. Rabah [13] investigated the potential syngas production of eight (8) livestock manures, namely, cattle dairy, cattle nondairy, sheep, goat, broiler, layer, horse, and camel. Li et al. [14] studied cow and sheep manures; Kaewtrakulchai et al. [15] investigated horse manure; and Tanczuk et al. [16] studied chicken manure. They established the range of the operating conditions as equivalent ratio ($ER = 0.01\text{-}1.0$), steam to biomass ratio ($SB = 0.0\text{-}3.0$), and gasification temperature ($T_g = 500^{\circ}\text{C-}1300^{\circ}\text{C}$).

FT synthesis demands syngas with an $H_2/CO \geq 2.0$ molar ratio for cobalt catalyst and $H_2/CO \approx 1.5$ for iron catalyst. Obtaining this molar ratio is not a straightforward process; it requires a special process. Despite the surging demand for diesel and gasoline, there is limited work oriented toward the production of syngas for FT synthesis. Buragohain et al. [2] developed a thermodynamic equilibrium model using a nonstoichiometric SOLGASMIX model for Gibbs energy minimization. The model has been tested with three types of biomass (sawdust, rice husk, and bamboo dust). The model is aimed at the production of syngas for power generation and FT synthesis. The syngas for power generation is required to have a maximum lower heating value (LHV), while the syngas for FT synthesis should have $H_2/CO \geq 2$. The optimum set of operating conditions for the gasifier for FT synthesis purposes has been established as $ER = 0.2\text{-}0.4$ and $T_g = 800\text{-}1000^{\circ}\text{C}$. The optimum set of operating conditions for the gasifier for power generation purposes has been found to be $ER = 0.3\text{-}0.4$ and $T_g = 700\text{-}800^{\circ}\text{C}$. Buragohain et al.'s [2] model was based on air as a gasification agent (i.e., no steam or air-steam mixture is used). This model produced two different types of syngas: one for power generation and one for FT synthesis.

As mentioned earlier, the paper reports an optimization model for thermal efficiency maximization constrained by FT synthesis requirements of $H_2/CO \geq 2.0$ molar ratio under a wide range of operating conditions (ER, SB, and T_g). The model is accomplished using the optimization section of the Model Analysis Tools of the Aspen Plus simulator. The model is optimized with the air-steam mixture as a gasification agent.

2. Model Development

The model's assumption, simulation, optimization, and sensitivity analysis are described in the following subsections. The model is accomplished using the sensitivity, optimization, and constraints sections of the Model Analysis Tools of the Aspen Plus simulator. The simulation model is tailored using the Aspen Plus guide [17].

2.1. Model Assumptions. The assumptions considered in the simulation are: (1) the key unit operations are biomass drying, pyrolysis, combustion and gasification, and gas cleaning. (2) The process is steady-state. (3) All vessels and reactors are at 1 bar and considered isobaric and adiabatic. (4) The feedstock is 10 kg/h on a dry and ash-free (DAF) basis. (5) Biomass is considered a nonreactive and nonconventional solid. (6) All gases are assumed to be ideal gas. (7) Air and steam are supplied at 1 bar. (7) The ambient temperature is 25°C. (8) Biomass is dried to 3% moisture at 1 bar and 150°C. (9) The product stream contains H_2, CO, CO_2, CH_4, N_2, H_2O, HCl, and H_2S. (10) The fluid package of the Peng-Robinson (PR-ROB) equation of state is selected to evaluate all physical properties of the conventional components. (11) The HCOALGEN and DCOALGEN property models are selected for the evaluation of the biomass formation enthalpy, specific heat capacity at constant pressure, and chemical density based on the proximate and ultimate analyses. (12) The chemical reactions are limited to reactions in Table 1, and (13) RStoic, RYield, and RGibbs reactors are selected for drying, pyrolysis, and gasification processes, respectively.

2.2. Process Simulation. Figure 1 shows the biomass gasification process flow diagram (PFD). The process description is attributed to Rabah [8] as below.

The wet biomass is fed into the "RStoic" reactor block (R-101), where moisture is liberated. The RStoic outlet stream (stream 2) goes into the separator (V-101), which separates the stream into moisture (stream 4) and dry biomass (stream 3). The dry biomass passes to the "RYield" reactor (R-102) for pyrolysis. The "RYield" reactor block calculates the yield distribution of the products without the need to specify reaction stoichiometry and reaction kinetics [18]. The "RYield" reactor converts biomass into conventional components (O_2, H_2, N_2, H_2O, S, tar, and char). The pyrolysis products (stream 5) are fed to the RGibbs reactor (R-103). The option of "Restrict chemical equilibrium-specify temperature approach or reactions" is chosen for the simulation of the RGibbs reactor. The reduction and oxidation reactions (Table 1) are supplied. The RGibbs reactor outlet (stream 6) moves to the cyclone (S-101), which separates stream 6 into wet syngas (stream 7) and ash (stream 8). The wet syngas (stream 7) is cooled in the heat exchanger (E-101), and the associated water is condensed. The cold wet syngas (stream 9) goes to the flash (V-102), which separates (stream 9) into syngas (stream 11) and water (stream 10). The air (stream 12) and steam (stream 13) as gasifying agents are added to the RGibbs reactor (R-103).

2.3. Model Optimization. The optimization process is conducted using the optimization section of the Model Analysis Tool of the Aspen Plus simulator. Optimization requires the definition of the objective function, the constraint, and the variables under which the objective function and constraint are satisfied. The optimization process is modeled below:

(1) *Objective Function*: the objective is the maximum thermal efficiency (η), which is defined by

$$\eta = \frac{\dot{Q}_o}{\sum \dot{Q}_i}, \tag{1}$$

Table 1: Biomass gasification chemical reactions [8].

Phase	Reaction name	Biomass gasification	ΔH_r [kJ/mole]
Drying		$Wet\ feedstock + heat = dry Feedstock + H_2O$	
Pyrolysis		Dry feedstock+heat = char+volatiles	
Oxidation	Combustion	$C + O_2 = CO_2$	-394
	Partial combustion	$C + 0.5O_2 = CO$	-111
	Combustion	$H_2 + 0.5O_2 = H_2O$	-242
Reduction	C-water reaction	$C + H_2O \leftrightarrow CO + H_2$	131
	Boudouard reaction	$C + CO_2 \leftrightarrow 2CO$	172
	C-Methanation	$C + H_2 \leftrightarrow CH_4$	-75
	Water gas shift	$CO + H_2O \leftrightarrow CO_2 + H_2$	-41
	Steam reforming	$CH_4 + H_2O \leftrightarrow CO + 3H_2$	206
		$S + H_2 = H_2S$	
		$Cl_2 + H_2 = 2HCL$	

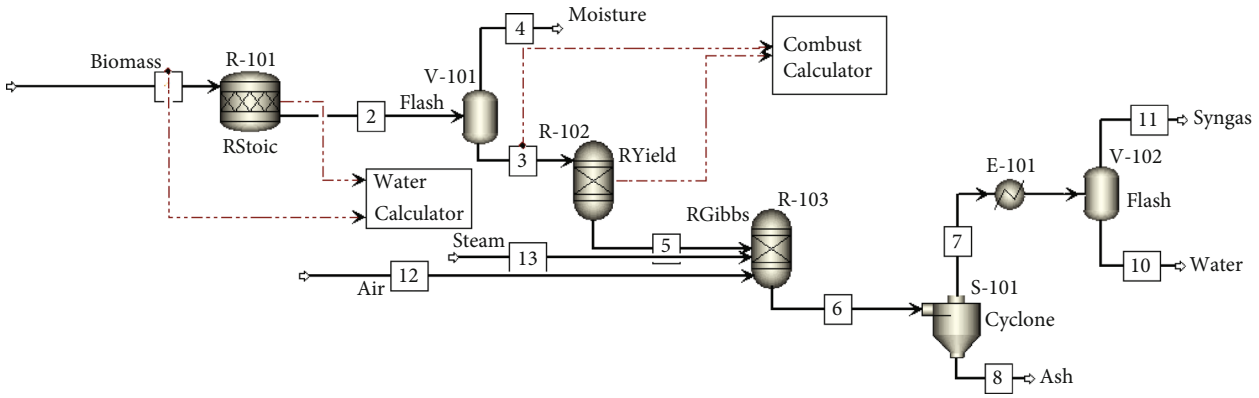

Figure 1: PFD of biomass gasification.

where $\dot{Q}_o$ is the syngas energy content and $\sum \dot{Q}_i$ is the sum of energy input for biomass drying ($\dot{Q}_1$), pyrolysis ($\dot{Q}_2$), air heating ($\dot{Q}_3$), steam generation ($\dot{Q}_4$), and biomass energy content ($\dot{Q}_5$). $\sum \dot{Q}_i$ also includes energy recovery from hot syngas ($\dot{Q}_6$), moisture ($\dot{Q}_7$), ash ($\dot{Q}_8$), and loss to the surrounding ($\dot{Q}_9$).

(a) The energy output with the syngas is calculated as

$$\dot{Q}_o = \dot{M}_o \mathrm{LHV}, \tag{2}$$

where $\dot{M}_o$ is the flow rate and LHV (MJ/kg) is the lower heating value of the syngas mass.

$$\mathrm{LHV} = \sum y_i \mathrm{LHV}_i,\ i = \mathrm{H_2}, \mathrm{CO}, \mathrm{CH_4}, \tag{3}$$

where y is the weight fraction. LHV for H_2, CO, and CH_4 are 120, 10, and 50 MJ/kg, respectively.

(b) Drying: the energy input to the dryer is used to heat the solid biomass ($\dot{Q}_b$) and evaporate water ($\dot{Q}_w$). Under a diabasic drying condition, the energy balance is [19]

$$\begin{aligned} \dot{Q}_1 &= \dot{Q}_b + \dot{Q}_w, \\ \dot{Q}_b &= \dot{M}_b \left(C_{pb} + \omega_i C_{pw}\right)\left(T_o - T_i\right), \\ \dot{Q}_w &= \dot{M}_b (\omega_i - \omega_o)\left(\lambda + \left(C_{pw} - C_{pv}\right) T_o\right), \end{aligned} \tag{4}$$

where $\dot{M}_b$ is the biomass flow rate. C_{pb}, C_{pw}, and C_{pv} are the specific heats of biomass, water, and water vapor. The specific heat of biomass is 0.42 kJ/kg K. T_i and T_o are ambient and drying temperatures. To ensure efficient moisture removal, the drying temperature is taken as $T_o = 150^{\circ}\mathrm{C}$. λ is the water's latent heat at 1 bar. ω_i and ω_o are the initial and final moisture content.

(c) Pyrolysis: the total heat requirement for pyrolysis is the sum of the sensible heat for the temperature rise of biomass to the reaction temperature and the heat of the reaction as

$$\dot{Q}_2 = \Delta H_b + \Delta H_r^o, \tag{5}$$

$$\Delta H_b = \dot{M}_b C_{pb}(T_r - T_i), \tag{6}$$

$$\Delta H_r^o = \dot{M}_b(553 - 3142x_{\text{char}}), \tag{7}$$

where x_{char} is the char concentration, $\dot{M}_b$ is the biomass flow rate, C_{pb} is the biomass-specific heat ($C_{pb} = 0.42\,\text{kJ/kg K}$), and T_r and T_i are the pyrolysis reactor and feed temperatures. The heat of the reaction is estimated based on the empirical equation (Equation (7)) of Antal [20].

(d) Air heating: the energy input for heating the air to gasification temperature is calculated using the first law of thermodynamics with zero work as

$$\dot{Q}_3 = \dot{M}_a Cp_a\left(T_g - T_i\right), \tag{8}$$

where $\dot{M}_a$ is the air mass flow rate, T_i is the ambient temperature, T_g is the gasification temperature, and Cp_a is the air-specific heat.

(e) Steam generation: the primary energy demand for steam generation is

$$\dot{Q}_4 = \dot{M}_s\left[C_{pw}(T_s - T_i) + \lambda + C_{pv}\left(T_g - T_s\right)\right], \tag{9}$$

where C_{pw} and C_{pv} are the specific heat of the water and water vapor. λ is the latent heat of evaporation. T_i, T_s, and T_g are the water inlet, steam saturation, and gasification temperatures, respectively. Steam generation is the major cost of biomass gasification.

(f) Biomass heating value: the biomass energy content is

$$\dot{Q}_5 = \dot{M}_b \text{HHV}. \tag{10}$$

HHV of biomass is calculated using Dulong's model given by

$$\text{HHV} = 81[C] + 342.5\left([H] - \frac{[O]}{8}\right) + 22.5[S], \tag{11}$$

where HHV is in kcal/kg ($1\,kcal/kg = 4.187\,kJ/kg$), and $[C]$, $[H]$, $[O]$, and $[S]$ are the concentration of carbon, hydrogen, oxygen, and sulfur, respectively (see Table 2).

(g) Energy recovery from syngas: syngas leaves the gasifier at a higher temperature and needs to be cooled prior to the gas cleaning step (moisture removal). The cooling medium is water in a heat exchanger E101. Hence, the energy recovery from syngas is

$$\dot{Q}_6 = \dot{M}_g C_{pg}\left(T_g - T_o\right), \tag{12}$$

where $\dot{M}_g$ is the syngas flow rate (including moisture), C_{pg} is the syngas-specific heat, and T_o is the syngas final temperature.

The energy input to pyrolysis is assumed to be integrated with energy recovery from the hot syngas in heat exchanger E101, energy escape with ash in cyclone S101, and moisture in the flash separator V101. This assumption is expected to make no significant error as steam generation and air heating are the major energy demands.

(2) *Constraint*: as noted earlier, the purpose of the present study is to optimize the operating conditions to produce syngas for FT synthesis. The principal chemical reactions for FT synthesis are:

$$\text{Synthesisofparaffin}: (2n+1)\text{H}_2 + n\text{CO} = C_nH_{(2n+2)} + n\text{H}_2\text{O}, \tag{13}$$

$$\text{Synthesisofolefins}: 2n\text{H}_2 + n\text{CO} = C_nH_{2n} + n\text{H}_2\text{O}. \tag{14}$$

The reactions given by Equations (13) and (14) show that H_2 and CO need to be in a stoichiometric ratio of 2 : 1 or higher. Therefore, we choose to produce syngas with excess hydrogen; hence, the following ratio is considered.

$$\frac{\text{H}_2}{\text{CO}} > 2.15. \tag{15}$$

(3) *Variables*: the objective function and the constraint are functions of type of biomass, (HHV) and syngas quality (LHV, H_2, CO CH_4 concentration). As noted in the literature review, the operating conditions of ER, SB, and T_g have a strong influence on syngas quality. These variables and their bounds are defined below.

ER is defined as the ratio of the actual and the stoichiometric air-fuel ratio (AFR) using the following

$$\text{ER} = \frac{(\text{AFR})_a}{(\text{AFR})_s} \tag{16}$$

where the subscripts a and s stand for actual and stoichiometric fuel-air ratio. AFR on a dry and ash-free basis (DAF) is calculated from ultimate analysis using the following:

$$\text{AFR} = \left(\frac{[C]}{12} + \frac{[H]}{4} + \frac{[S]}{32} - \frac{[O]}{32}\right)\left(1 + \frac{79}{21}\right)\left(1 - \frac{[Ash]}{100}\right)\frac{28.4}{100}. \tag{17}$$

Table 2: MSW proximate and ultimate analyses, AFR, and SB on DAF basis.

MSW	Ref.	Moisture	Proximate			Ultimate						HHV	AFR	SB
			FC	VM	Ash	C	H	O	N	S	Cl			
			%									MJ/kg		
MSW01	[21]	12.00	15.47	38.29	46.24	36.40	4.97	10.15	1.44	0.80	0.00	17.77	2.92	0.29
MSW02	[22]	48.00	7.70	46.15	46.15	30.77	4.62	17.30	0.77	0.39	0.00	14.02	2.35	0.25
MSW03	[23]	20.00	10.70	77.60	11.70	47.90	6.00	32.90	1.20	0.30	0.00	19.00	5.41	0.63
MSW04	[24]	20.00	12.82	77.66	9.51	43.71	7.74	36.69	1.95	0.40	0.00	19.42	5.51	0.59
MSW05	[25]	30.90	8.40	79.10	12.50	47.81	5.18	31.37	1.62	0.81	0.71	18.11	5.17	0.63
MSW06	[25]	36.00	8.80	82.90	8.30	45.14	4.86	37.75	2.53	0.81	0.61	15.59	4.78	0.62
MSW07	[25]	34.40	7.40	84.00	8.60	50.15	5.13	32.25	2.62	0.84	0.42	18.67	5.59	0.69
MSW08	[26]	52.70	16.00	73.00	11.00	46.20	6.10	34.80	1.30	0.10	0.50	18.21	5.24	0.62
MSW09	[27]	20.00	18.84	80.00	1.16	51.19	6.08	41.30	0.20	0.02	0.05	18.69	6.10	0.76
MSW10	[28]	8.04	16.76	77.41	5.83	45.64	6.20	39.53	1.40	0.24	1.16	17.31	5.32	0.64
MSW11	[29]	3.30	7.50	83.02	9.48	57.98	7.47	24.62	0.36	0.09	0.00	26.01	7.37	0.79

The steam to biomass ratio (SB) is defined as

$$SB = \frac{\text{Feedof}H_2O\text{assteam[kg/h]}}{\text{Flowofbiomass[kg/h]}}. \quad (18)$$

Stoichiometric steam to biomass ratio (SB) is

$$SB = \left(\frac{[C]}{12}\right)\left(1 - \frac{[\text{Ash}]}{100}\right)\frac{18}{100}. \quad (19)$$

(4) Variable bounds: the following bounds of the operating conditions are considered.

$$\begin{cases} 0 \leq & ER & \leq 1.0, \\ 0 \leq & \text{SB} & \leq 5.0, \\ 500 \leq & T & \leq 1300 \circ \text{C}. \end{cases} \quad (20)$$

2.4. Sensitivity Analysis. A parametric sensitivity analysis is performed to investigate the influence of the operating conditions (ER, SB, and T_g) on syngas quality. These operating conditions have the most influence on the gasification process. The sensitivity section of the Model Analysis Tools of the Aspen Plus simulator is run for the same range of ER, SB, and T_g considered in the optimization model. The performance is assessed with four measures, viz., syngas molar concentration of CO, CO_2, H_2, and CH_4; thermal efficiency; LHV; and H_2/CO molar ratio.

3. Results and Discussions

3.1. Material Characteristics. Table 2 shows eleven MSWs, randomly selected from different sources. The selected MSWs have been used previously in simulation and experimental gasification research. The main characteristics of MSW are moisture, proximate and ultimate analyses, and HHV. The major components of MSW are organic, paper, plastic, metal, glass, and others (electric light, batteries, automotive parts, medicines, and chemicals). MSW characteristics depend on its composition and vary from community to community.

HHV is a function of carbon, hydrogen, and sulfur content as given by Equation (11). Carbon is the major component of biomass, followed by hydrogen and sulfur. Hydrogen has the highest calorific value of 120 MJ/kg, followed by carbon (33.74 MJ/kg) and sulfur (9.3 MJ/kg). The carbon content for MSW ranges from 31 to 58% by weight, while hydrogen and sulfur account for less than 8 and 1 percent by weight, respectively. Not all carbon is available for heat, because oxygen partially oxidized the carbon, decreasing its ability to generate heat. Similarly, not all hydrogen is available for heat because part of the hydrogen combines with oxygen to form water vapor according to the combustion reaction ($H_2 + 0.5O_2 = H_2O$). The hydrogen available for heat is thus ($[H] - ([O])/8$). Hence, the higher the carbon and hydrogen contents the higher the heating value, and the higher the oxygen content the lower the heating value. MSW11 has HHV close to that of coal (25 to 35 MJ/kg) because of its higher carbon and hydrogen and lower oxygen content relative to other MSWs.

Table 2 shows AFR, and SB was calculated using Equations (16)–(19) on a DAF basis. The calculated AFR is based on the complete combustion of all biomass. In gasification, complete combustion is needed only to meet the energy demand for endothermic reduction reactions. Hence, ER should be minimum ($ER < 1$) to avoid complete combustion. SB is calculated based on the C-water reaction ($C + H_2O = CO + H_2$). In gasification, besides the C-water reaction, steam is required for water gas shift ($CO + H_2O = H_2 + CO_2$) and steam reforming ($CH_4 + H_2O = CO + 3H_2$) reactions. Hence, the actual SB should be higher than the stoichiometric value shown in Table 2.

3.2. Model Validation. The results of the simulation model are compared with the simulation data of Suwatthiku et al. [30] at the same operating conditions (ER, SB, and T_g). The relative error is estimated as

$$E_i = \left| \frac{y_{ai} - y_{bi}}{y_{bi}} \right|, \quad (21)$$

where y is the mole fraction of syngas composition (H_2, CO, CO_2, and CH_4). The subscripts a and b stand for the present and Suwatthiku et al.'s [30] works, respectively. i is the counter and n is the total number of points. The mean square error (MSE) and the root mean square error (RMSE) are estimated using Equations (22) and (23).

$$\text{MSE} = \frac{1}{n} \sum_{1}^{n} E_i^2, \quad (22)$$

$$\text{RMSE} = \sqrt{\text{MSE}}. \quad (23)$$

Table 3 shows the proximate and ultimate analyses of the biomass used for comparison with Suwatthiku et al.'s [30] simulation.

Table 4 shows the operating conditions (ER, SB, and T_g), the present and Suwatthiku et al.'s [30] simulation results, and the statistical parameters. Besides (H_2, CO, CO_2, CH_4), syngas also contains H_2O and traces of N_2, H_2S, and HCl. However, for the sake of comparison, the syngas composition is normalized to (H_2, CO, CO_2, and CH_4). The present work predicts Suwatthiku et al.'s [30] results with a RMSE of 0.20, 0.23, 0.39, and 1.0 for H_2, CO, CO_2, and CH_4, respectively. It can be observed that the present results are in good agreement with Suwatthiku et al.'s [30] results for the case of H_2, CO, and CO_2 and in poor agreement with CH_4. The poor match for the case of CH_4 is attributed to the fact that the minimum formation of methane is a common problem experienced by many simulations works [8, 31].

3.3. Optimization Results. Table 5 shows the optimization results. It includes the following information:

(1) Optimal operating conditions (ER, SB, T_g) and efficiency

(2) Syngas characteristics: compositions (H_2, CO, CO_2, CH_4, N_2, H_2O, H2S, and HCl) and thermophysical properties (ρ, MW, and LHV)

(3) Other variables: biomass flow rate ($\dot{M}_b$), syngas flow rate ($\dot{M}_o$), yield, and biomass used as a fuel (Δ)

(i) Compositions are in mole % except CH_4, H_2S, and HCL are in ppm. (ii) All parameters have usual SI units. (iii) $Y = Yield = \dot{M}_o/\dot{M}_b$, where $\dot{M}_o$ and $\dot{M}_b$ are the syngas and biomass mass flow rates, respectively. (iv) η and Δ are in %.

3.3.1. Optimal Operating Conditions

(1) Equivalent Ration (ER). The optimization returned ER = 0, indicating no external air is needed. There are mainly three sources of oxygen for combustion reaction, viz., biomass, steam, and external air. The oxygen in the biomass is between 10% and 40% (see Table 2). Steam contains 89% oxygen and 11% hydrogen (oxygen contribution by water molecules). These two sources provide adequate oxygen for the partial combustion reaction. The advantages of $ER = 0$ are zero energy input for air and minimum nitrogen in the syngas.

(2) Steam to Biomass Ratio (SB). Table 5 shows SB for different types of MSW. The optimum SB is $0.66 \le SB \le 1.22$. Chang et al. [32] and Molino et al. [33] reported the optimal SB value in the range of 0.3-1.0. The main sources of steam are steam input, moisture content, and steam generated in the combustion reaction ($H_2 + 0.5O_2 \leftrightarrow H_2O$). The steam is consumed in C-water, water gas shift, and steam reforming reactions. The advantage of steam gasification is the enhancement of H_2 and LHV in syngas. In practice, the energy input for steam generation is supplied by biomass as a fuel. Hence, it is important to estimate the percentage of biomass used as a fuel in steam generation. This is estimated as:

$$\Delta_s = \frac{\dot{Q}_4}{\eta_b \dot{Q}_5} \times 100\%, \quad (24)$$

where Δ is the % of biomass used as fuel in steam generation, η_b is the boiler efficiency, $\dot{Q}_4$ is the energy input with steam (see Equation (9)), and $\dot{Q}_5$ is the energy input with biomass (see Equation (10)). With a boiler efficiency of 80%, the biomass fuel for steam generation is $\Delta_s = 7.16$-22.69% of the total biomass.

Likewise, the biomass used as a fuel for drying is

$$\Delta_d = \frac{\dot{Q}_1}{\eta_b \dot{Q}_5} \times 100\%, \quad (25)$$

and for pyrolysis is

$$\Delta_p = \frac{\dot{Q}_2}{\eta_b \dot{Q}_5} \times 100\%. \quad (26)$$

With dryer and pyrolysis thermal efficiency of 80%, the biomass used a fuel for drying and pyrolysis *are* $\Delta_d = 0.38$ -16.48% and $\Delta_p = 0.75$-4.11% of the total biomass, respectively. The total biomass used as fuel for steam generation, drying, and pyrolysis is in the range of 12.98%-33.12% (see Table 2).

(3) Gasification Temperature T_g. The optimal gasification temperature is $T_g = 679$-763°C. Pala et al. [3] reported $T_g = 800$ -900°C. Buragohain et al. [2] reported the optimal conditions for the gasifier for FT synthesis purposes as $T_g = 800$-1000°C. The present work returned significantly lower T_g than Buragohain et al.'s [2] model. However, it is noted that the previous research used air as the gasification medium, i.e., $SB = 0$. This justifies the high gasification temperature of the previous works. Lower T_g tends to lower energy consumption, tar, and NO_x formation.

Table 3: Validation biomass sample.

Moisture	Proximate			Ultimate				
	VM	FC	Ash	C	H	O	N	S
8.00	82.29	17.16	0.55	50.54	7.08	41.11	0.15	0.57

Table 4: Validation results.

ER	SB	T_g	H_2			CO			CO_2			CH_4		
			x_a	x_b	E	x_a	x_b	E	x_a	x_b	E	x_a	x_b	E
0.00	8.9	916	0.57	0.56	0.01	0.39	0.29	0.35	0.04	0.10	0.59	0.00	0.05	0.99
0.04	8.9	936	0.56	0.54	0.04	0.39	0.31	0.28	0.05	0.12	0.59	0.00	0.04	1.00
0.09	8.9	949	0.55	0.51	0.08	0.39	0.32	0.22	0.06	0.13	0.57	0.00	0.04	1.00
0.00	17.8	856	0.60	0.56	0.08	0.29	0.29	0.02	0.11	0.09	0.24	0.00	0.07	1.00
0.04	17.8	814	0.60	0.53	0.13	0.28	0.31	0.09	0.12	0.11	0.10	0.00	0.05	0.99
0.09	17.8	884	0.58	0.49	0.20	0.29	0.33	0.10	0.12	0.14	0.11	0.00	0.05	1.00
0.13	17.8	898	0.58	0.49	0.19	0.29	0.33	0.11	0.13	0.14	0.09	0.00	0.04	1.00
0.18	17.8	911	0.57	0.47	0.21	0.30	0.34	0.13	0.13	0.15	0.12	0.00	0.04	1.00
Min					0.01			0.02			0.09			0.99
Max					0.21			0.35			0.59			1.00
MSE					0.04			0.05			0.15			0.99
RMSE					0.20			0.23			0.39			1.00

(4) Efficiency. Table 5 shows the gasification efficiency estimated using Equation (1). The major energy consumption processes are drying, pyrolysis, and gasification. The minimum and maximum efficiency are 49% and 85% for MSW1 to MSW9. However, MSW10 and MSW11 experienced abnormally high efficiencies of 93% and 94%, respectively. This could be attributed to the low moisture content of MSW10 (8.03%) and MSW11 (3.30%); the moisture content of MSW1 to MSW9 is in the range of 12-52% (see Table 2).

3.3.2. Syngas Quality

(1) Syngas Composition. Syngas composition is shown in Table 5. The major syngas compositions are H_2, CO, and CO_2. The optimization returned zero concentrations of S and Cl_2, C, and O_2, and traces (in ppm) of CH_4, H_2S, and HCl. The hydrogen concentration varies between 52.38% and 58.67%. The hydrogen sources are hydrogen in the feedstock is 4.62-7.74% (Table 2), hydrogen that comes through steam (steam consists of 11% hydrogen and 89% oxygen), and hydrogen generated through C-water, water gas shift, and steam reforming reactions. The hydrogen is depleted by combustion reaction ($H_2 + 0.5O_2 \leftrightarrow H_2O$), C-methylation reaction ($C + H_2 = CH_4$), and reaction with S ($S + H_2 \leftrightarrow H_2S$) and ($Cl_2 + H_2 \leftrightarrow 2HCl$). The high concentration of H_2 is thus may attribute to no occurrence of combustion and C-methylation reactions. The CO concentration varies between 24.36 and 27.27% which is significantly higher than CO_2. The main sources of CO are partial combustion, C-water, Boudouard, and steam reforming reactions. The main CO delation reaction is the water gas shift reaction. The high CO concentration may be attributed to the high conversion of the CO production reaction and the backward shift of the water gas reaction to reactants. The CO_2 concentration varies between 6.21 and 14.74%. The source of CO_2 is combustion and the water gas shift reaction. CO_2 is depleted by Boudouard's reaction. Clearly, the low concentration of CO_2 may be attributed to high conversion by Boudouard's reaction and the backward shift of the water gas shift reaction. Zero concentration of S and Cl_2 is due to complete conversion into H_2S and HCl. Zero concentrations of C and O_2 are indicative to complete the conversion of C into CO and CO_2. The low concentration of CH_4 may be attributed to the high conversion of the steam reforming reaction.

3.4. Sensitivity Analysis. As indicated earlier, the performance of the gasification process has been assessed with two measures, viz., syngas molar concentration (CO, CO_2, H_2, and CH_4), efficiency, and H_2/CO molar ratio. The influence of T_g, SB, and ER on these performance measures is presented. A sample of the results is discussed in the following subsections; the rest of the results (not shown here) show the same.

3.4.1. Influence of T_g on Syngas Quality. Figure 2 shows the influence of T_g on CO, CO_2, H_2, and CH_4 mole fraction in the range of 500°C-1300°C at constant ER and SB. As T_g increases, CO and CO_2 assume opposite trends and reach a point of crossover. The decrease in CO_2 could be attributed to the Boudouard reaction and the deficiency of O_2 for complete combustion reactions (see Table 1). The increase in CO is attributed to partial combustion, C-water, Boudouard, and steam reforming reactions. The point of crossover is known

Table 5: Optimization results.

MSW	1	2	3	4	5	6	7	8	9	10	11	Min	Max
Operating conditions and variables													
ER	0.00	0.00	0.00	0.01	0.00	0.00	0.00	0.00	0.00	0.00	0.00	0.00	0.01
SB	1.22	0.93	0.86	0.66	1.00	0.87	1.03	0.89	0.88	0.82	1.08	0.66	1.22
T_g	763	761	679	745	714	709	712	740	710	750	695	679	763
$\dot{M}_i$	21.14	35.71	14.16	13.81	16.54	17.04	16.68	23.75	12.65	11.55	11.42	11.42	35.71
$\dot{M}_o$	21.53	18.24	17.17	16.10	17.96	16.48	18.14	16.90	16.74	16.01	19.72	16.01	21.53
η	84.87	50.09	79.77	79.77	69.09	64.85	65.86	47.83	81.56	92.82	94.60	47.83	94.60
Y	1.02	0.51	1.21	1.17	1.09	0.97	1.09	0.71	1.32	1.39	1.73	0.51	1.73
Biomass % used as fuel for steam generation, drying, and pyrolysis													
Δ_s	8.46	7.16	18.29	17.10	18.09	17.90	19.82	17.78	21.88	18.58	22.69	7.16	22.69
Δ_d	2.98	16.48	4.87	4.77	8.09	11.01	8.77	13.97	4.95	1.93	0.38	0.38	16.48
Δ_p	1.53	4.11	2.42	1.94	3.03	3.42	3.15	1.38	0.75	1.28	2.25	0.75	4.11
Δ_t	12.98	27.76	25.58	23.81	29.21	32.33	31.74	33.12	27.58	21.79	25.33	12.98	33.12
Syngas compositions													
H_2	58.67	57.92	53.03	55.96	54.01	52.38	53.63	55.49	54.05	54.86	55.51	52.38	58.67
CO	27.27	26.94	24.62	26.04	25.09	24.36	24.91	25.80	25.13	25.50	25.81	24.36	27.27
CO_2	6.21	7.78	12.58	8.62	12.64	14.74	13.00	11.27	13.45	12.12	9.29	6.21	14.74
CH_4	6993	5336	29620	6585	9679	8238	9526	5347	10038	3355	29784	3355	29784
H_2O	6.28	6.28	6.29	6.28	6.29	6.29	6.29	6.28	6.29	6.28	6.28	6.28	6.29
N_2	0.58	0.38	0.43	2.33	0.56	0.96	0.87	0.45	0.07	0.50	0.10	0.07	2.33
O_2	0.00	0.00	0.00	0.00	0.00	0.00	0.00	0.00	0.00	0.00	0.00	0.00	0.00
H_2S	2814	1674	942	1210	2456	2683	2438	305	58	747	221	57	2814
HCL	0.00	0.00	0.00	0.00	1947	1828	1103	1379	131	3268	0.00	0.00	3267
S	0.00	0.00	0.00	0.00	0.00	0.00	0.00	0.00	0.00	0.00	0.00	0.00	0.00
CL_2	0.00	0.00	0.00	0.00	0.00	0.00	0.00	0.00	0.00	0.00	0.00	0.00	0.00
C	0.00	0.00	0.00	0.00	0.00	0.00	0.00	0.00	0.00	0.00	0.00	0.00	0.00
H_2/CO	2.15	2.15	2.15	2.15	2.15	2.15	2.15	2.15	2.15	2.15	2.15	2.15	2.15
Syngas thermophysical properties													
ρ	0.50	0.52	0.59	0.54	0.59	0.62	0.59	0.57	0.59	0.58	0.54	0.50	0.62
MW	13.06	13.52	15.26	14.14	15.28	16.06	15.43	14.71	15.37	15.05	14.08	13.06	16.06
LHV	17.15	16.26	14.48	15.10	13.66	12.55	13.42	14.33	13.61	13.74	16.36	12.55	17.15

as the carbon boundary point (CBP), the point where carbon is depleted. Similar trends and CBP have been reported by Pala et al. [3], Rabah [8], Rabah [13], Begum et al. [10], and Safarian et al. [34]. As T_g increases, H_2 increases to a maximum point at $T_g \approx 760^{\circ}C$ and then slightly reverses downward. The decrease in the hydrogen content with increasing temperature is likely to be due to the shifting of the exothermic water gas shift ($CO + H_2O \leftrightarrow CO_2 + H_2$) toward reactants. CH_4 is depleted with increasing temperature. CH4 is produced by the C-methanation reaction and depleted by steam reforming relations. The same results have been observed for the remaining feedstock (not shown here).

Figure 2(a) shows the influence of T_g on LHV, efficiency, and the H_2/CO molar ratio. These three parameters are influenced by H_2, CO, and CH_4 concentrations. The efficiency profile increases, then decreases, similar to the H_2 profile. LHV decline is continuous, similar to the CH_4 profile. The decline in H_2/CO is due to the increasing formation of CO. Excessively high gasification temperature ($T_g \geq 1000^{\circ}C$) tends to reduce the H_2/CO molar ratio, LHV, and increase energy consumption, tar, and NO_x formation.

3.4.2. Influence of SB on Syngas Quality. Figure 3(a) shows the influence of SB on CO, CO_2, H_2, and CH_4 mole fraction at constant ER and T_g. CO and CH_4 mole fractions are decreasing, while CO_2 and H_2 mole fractions are increasing with increasing SB. As SB increases, steam will be available for water gas shift and steam reforming reactions to convert CO and CH_4 into CO_2 and H_2 (see Table 1). The point where CO and CO_2 crossover is known as the carbon boundary point (CBP), as mentioned earlier. Figure 3(b) shows LHV, efficiency, and H_2/CO versus SB. H_2/CO

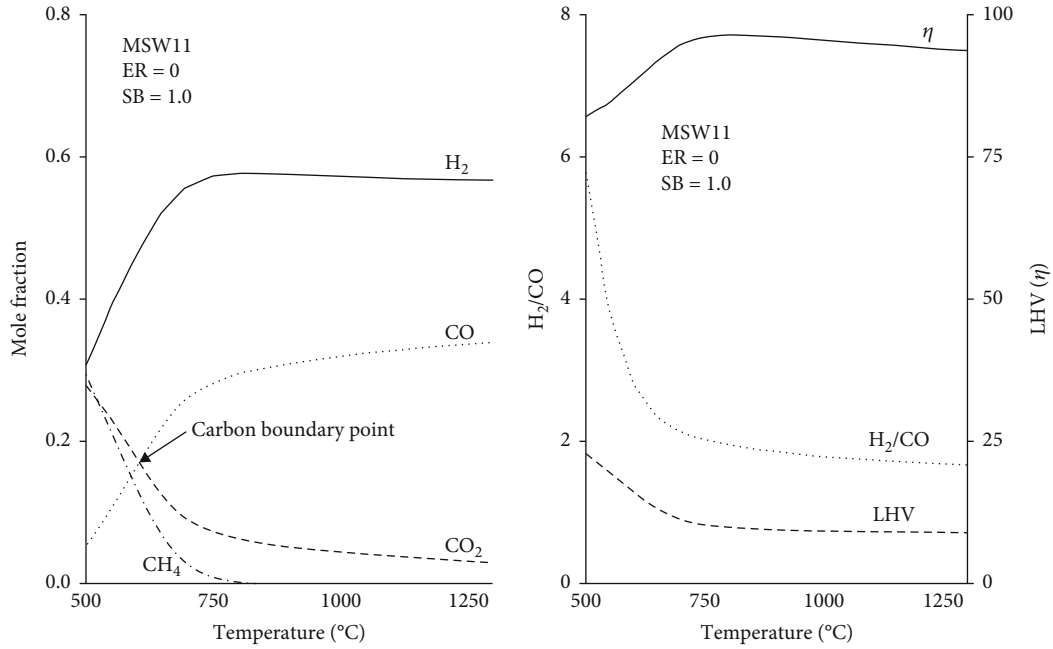

(a) Composition (b) Efficiency and H_2/CO. η and H_2/CO on the secondary axis

Figure 2: Influence of temperature on composition, efficiency, and H_2/CO.

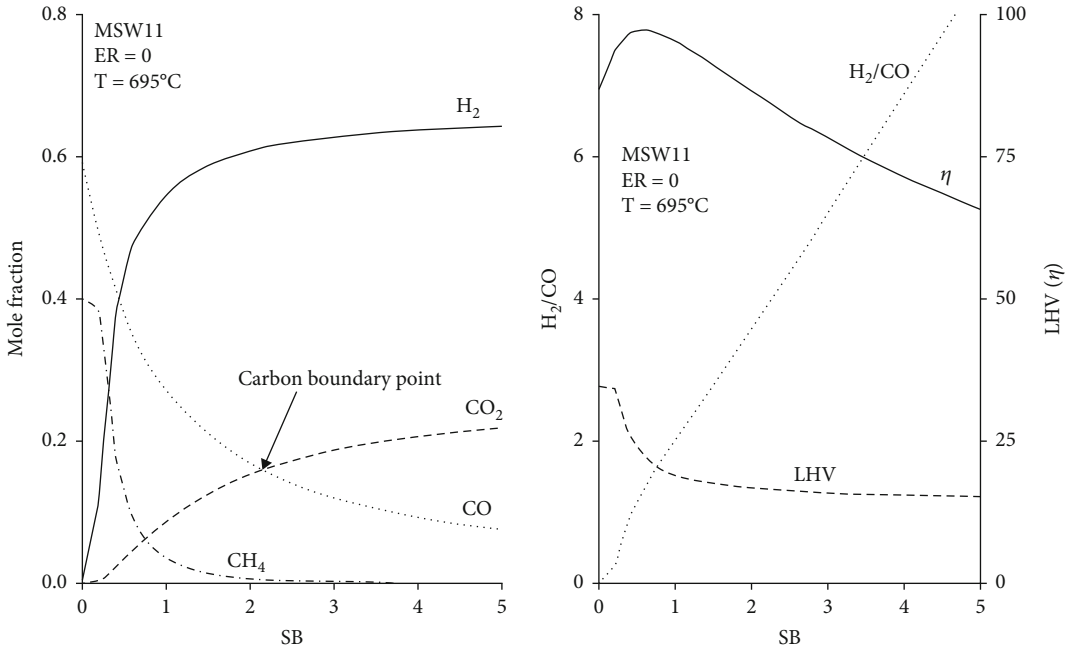

(a) Concentration (b) Efficiency and H_2/CO. η and H_2/CO on the secondary axis

Figure 3: Influence of SB on composition, efficiency, and H_2/CO.

assumes a positive linear variation with SB. At $SB = 1.0$, maximum efficiency and $H_2/CO \geq 2$ occur, which is consistent with optimization results.

3.4.3. Influence of ER on Syngas Quality. Figure 4(a) shows the influence of ER on the CO, CO_2, H_2, and CH_4 mole fractions at constant SB and T_g. The H_2, CO, and CH_4 mole fractions are decreasing with increasing ER, but CO_2 is increasing. This is expected, as more O_2 is available, complete combustion occurs, converting C to CO_2. CO and CO_2 crossovers occur at $ER = 0.25$. Similar trends have been reported by Pala et al. [3], Rabah [8], Begum et al. [10], and

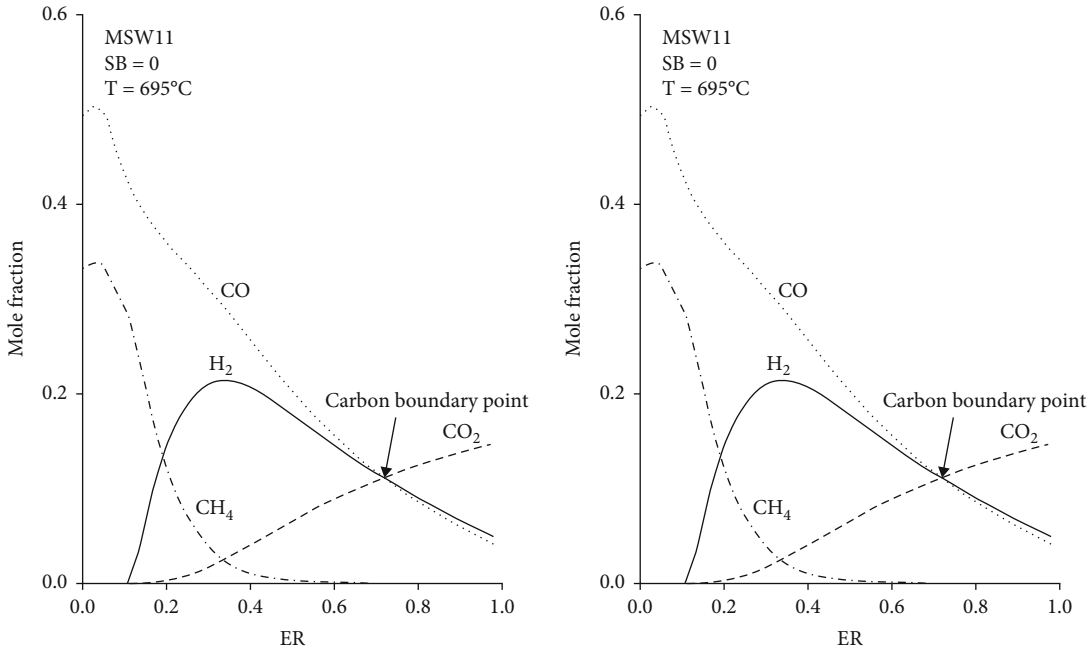

(a) Concentration

(b) Efficiency and H_2/CO. η and H_2/CO on the secondary axis

Figure 4: Influence of ER on composition, efficiency, and H_2/CO.

Safarian et al. [34]. Figure 4(b) shows LHV, efficiency, and H_2/CO versus ER. Clearly, as more O_2 is available and the process is complete combustion and not biomass gasification process, it can be concluded that pure air gasification does not produce syngas quality that meets the FT synthesis requirement of $H_2/CO \geq 2.15$. In addition, air gasification increases energy consumption and N_2 in syngas [31].

4. Conclusion

This work reports the results of the optimization model of biomass gasification, aimed to produce syngas for use as a feedstock for FT synthesis. The model is accomplished using the optimization section of the Model Analysis Tools of the Aspen Plus simulator. The thermal efficiency is maximized under the constraint of $H_2/CO \geq 2.15$ molar ratio and the variables of $SB = 0.0$-5.0, $ER = 0.0$-1.0, and $T_g =$ 500-1000°C. The simulation model is validated with the results obtained from the literature. The performance measures considered are syngas quality, thermal efficiency, LHV, and H_2/CO≥ molar ratio. The optimum operating conditions and syngas quality for eleven (11) types of MSW are made available. The optimum operating conditions have been found as $ER = 0$, $SB = 0.66$-1.22, and $T_g = 679$-763°C. Under the optimum operating conditions, a high-quality syngas has been produced with characteristics of $H_2 = 52.38$ -58.67%v/v and $N_2 = 0.38$-$2.33\%v/v$, $H_2/CO \geq 2.15$, and $LHV = 12.55$-17.15 MJ/kg, and zero NO_x formation. The reported generalized optimization model is applicable to all types of biomass and coal.

Nomenclature

Roman Letters

AFR: Stichometric air-fuel ratio
C_p: Isobaric specific heat capacity (kJ/kg K)
DAF: Dry and ash-free basis
E: Relative error
ER: Equivalence ratio
FC: Fixed Carbon
h: Enthalpy (kJ/kg K)
HHV: Higher heating value (MJ/kg)
LHV: Lower heating value (MJ/kg)
$\dot{M}$: Mass flow rate (kg/s)
max: Maximum
min: Minimum
MSE: Mean square error
MSW: Municipal solid waste
MW: Molecular weight (kg/kmole)
RMSE: Root mean square error
$\dot{Q}$: Heat transfer rate
SB: Steam to biomass ratio
toe: Ton of oil equivalent
T: Temperature (°C)
VM: Volatile matter
y: Gas mole fraction
Y: Yield.

Greek Letters

η: Thermal efficiency

Δ: Biomass % used as fuel for steam generation, drying, and pyrolysis (%)
λ: Latent heat of vaporization (kJ/kg)
ω: Moisture fraction.

Subscripts

b: Biomass
d: Drying
i: Index 1,2,3,..., input
p: Pyrolysis
o: Output
s: Steam
t: Total
w: Water
v: Vapor.

Superscript

$^\circ$: Degree.

Data Availability

All information used to support the findings of the study are available from the corresponding author upon request.

Disclosure

The author conducted this work as part of his normal research activities as a professor of Chemical Engineering at theUniversity of Khartoum, Sudan.

Conflicts of Interest

The author declares that he has no conflicts of interest.

References

[1] U. J. Siregar, A. Lestari, L. Rusniarsyah, and C. A. Siregar, "Fuel substitution by wood gasification for diesel electricity generator," *IOP Conference Series: Materials Science and Engineering*, vol. 935, no. 1, article 012048, 2020.

[2] B. Buragohain, P. Mahanta, and V. S. Moholkar, "Thermodynamic optimization of biomass gasification for decentralized power generation and Fischer-Tropsch synthesis," *Energy*, vol. 35, no. 6, pp. 2557–2579, 2010.

[3] L. P. R. Pala, Q. Wang, G. Kolb, and V. Hesse, "Steam gasification of biomass with subsequent syngas adjustment using shift reaction for syngas production: an Aspen Plus model," *Renewable Energy*, vol. 101, no. 2017, pp. 484–492, 2017.

[4] M. Martin and I. E. Grossmann, "Process optimization of FT-diesel production from lignocellulosic switchgrass," *Industrial and Engineering Chemistry Research*, vol. 50, no. 23, pp. 13485–13499, 2011.

[5] IEA, "Enerdata: World Energy and Climate Statistics (2020)," 2021, http://www.iea.org/reports/key-world-energy-statistics-2020/final-consumption.

[6] B. Lamolinara, A. Pérez-Martínez, E. Guardado-Yordi, C. G. Fiallos, K. Diéguez-Santana, and G. J. Ruiz-Mercado, "Anaerobic digestate management, environmental impacts, and techno-economic challenges," *Waste Management*, vol. 140, pp. 14–30, 2022.

[7] M. Balat and G. Ayar, "Biomass energy in the world, use of biomass and potential trends," *Energy Sources*, vol. 27, no. 10, pp. 931–940, 2005.

[8] A. Rabah, "Syngas production from agriculture residues: Sudan," *Journal of Energy*, vol. 2022, Article ID 2944552, 10 pages, 2022.

[9] S. Beguma, M. G. Rasula, and D. Akbarb, "A numerical investigation of municipal solid waste gasification using Aspen Plus," *Procedia Engineering*, vol. 90, pp. 710–717, 2014.

[10] S. Begum, M. Rasul, D. Akbar, and N. Ramzan, "Performance analysis of an integrated fixed bed gasifier model for different biomass feedstocks," *Energies*, vol. 6, no. 12, pp. 6508–6524, 2013.

[11] A. Hlavsová, A. Corsaro, H. Raclavská, D. Juchelková, H. Škrobánková, and J. Frydrych, "Syngas production from pyrolysis of nine composts obtained from nonhybrid and hybrid perennial grasses," *The Scientific World Journal*, vol. 2014, Article ID 723092, 11 pages, 2014.

[12] M. Alex, "A comparison of prairie cordgrass and switchgrass as a biomass for syngas production," *Fuel*, vol. 95, pp. 573–577, 2012.

[13] A. A. Rabah, "Livestock manure availability and syngas production: a case of Sudan," *Energy*, vol. 259, no. 15, article 124980, 2022.

[14] Y. Li, S. Achinas, J. Zhao, B. Geurkink, J. Krooneman, and G. J. Willem Euverink, "Co-digestion of cow and sheep manure: performance evaluation and relative microbial activity," *Renewable Energy*, vol. 153, pp. 553–563, 2020.

[15] N. Kaewtrakulchai, A. Putta, W. Pasee, K. Fuangnawakij, G. Panomsuwan, and A. Eiad-ua, "Magnetic carbon nanofibers from horse manure via hydrothermal carbonization for methylene blue adsorption," *Materials Science and Engineering*, vol. 540, no. 1, article 012006, 2019.

[16] M. Tańczuk, R. Junga, A. Kolasa-Więcek, and P. Niemiec, "Assessment of the energy potential of chicken manure in Poland," *Energies*, vol. 12, no. 7, p. 1244, 2019.

[17] Aspentech, *Aspen Plus: getting started modeling processes with solids*, Burlington, USA, 2013.

[18] F. Paviet, F. Chazarenc, and M. Tazerout, "Thermo chemical equilibrium modelling of a biomass gasifying process using Aspen Plus," *International Journal of Chemical Reactor Engineering*, vol. 7, no. 1, pp. 1–16, 2009.

[19] Z. B. Marouslis, S. A. Mujumdar, and G. D. Saravcos, "Spreadsheetaider dryer design," in *Hand Book of Industerial Drying*, Tylor And Francis Group, London, 2006.

[20] M. Antal Jr., "Biomass pyrolysis," in *A review of the literature Part 1- carbohydate pyrolysis'*, Advances in Solar Energy, K. Böehr and J. Duffie, Eds., pp. 61–111, Springer, New York, 1985.

[21] S. Naveed, A. Malik, N. Ramzan, and M. Akram, "A comparative study of gasification of food waste (FW), poultry waste (PW), municipal solid waste (MSW) and used tires (UT)," *Nucleus*, vol. 46, pp. 77–81, 2009.

[22] C. Chen, Y. Q. Jin, J. H. Yan, and Y. Chi, "Simulation of municipal solid waste gasification in two different types of fixed bed reactors," *Fuel*, vol. 103, pp. 58–63, 2013.

[23] M. Oliveira, A. Ramosb, E. Monteiroc, and A. Abel Rouboab, "Modeling and simulation of a fixed bed gasification process for thermal treatment of municipal solid waste and agricultural residues," *Energy Reports*, vol. 7, no. 2021, pp. 256–269, 2021.

[24] P. A. Sesotyo, M. Nur, and J. E. Suseno, "Plasma gasification with municipal solid waste as a method of energy self sustained for better urban built environment: modeling and simulation," *Science*, vol. 396, no. 1, article 012002, 2019.

[25] L. Makarichi, R. Kan, W. Jutidamrongphan, and K. Techato, "Suitability of municipal solid waste in African cities for thermochemical waste-to-energy conversion: the case of Harare Metropolitan City, Zimbabwe," *Waste Management and Research*, vol. 37, no. 1, pp. 83–94, 2019.

[26] T.-H. Kwak, S. Lee, J.-W. Park, S. Maken, Y. D. Yoo, and S.-H. Lee, "Gasification of municipal solid waste in a pilot plant and its impact on environment," *Korean Journal of Chemical Engineering*, vol. 23, no. 6, pp. 954–960, 2006.

[27] W. Doherty, A. Reynolds, and D. Kennedy, "Aspen Plus simulation of biomass gasification in a steam blown dual fluidised bed," in *Materials and processes for energy: communicating current research and technological developments*, A. Méndez-Vilas, Ed., Formatex Research Centre, 2013.

[28] A. D. Pasek, K. W. Gultom, and A. Suwono, "Feasibility of recovering energy from municipal solid waste to generate electricity," *Journal of Engineering and Technological Sciences*, vol. 45, no. 3, pp. 241–256, 2013.

[29] M. Azama, S. S. Jahromya, W. Razab et al., "Status, characterization, and potential utilization of municipal solid waste as renewable energy source: Lahore case study in Pakistan," *Environment International*, vol. 134, article 105291, 2020.

[30] A. Suwatthiku, S. Limprachaya, P. Kittisupakorn, and I. M. Mujtaba, "Simulation of steam gasification in a fluidized bed reactor with energy self-sufficient condition," *Energies*, vol. 10, no. 3, pp. 314–329, 2017.

[31] W. Doherty, A. Reynolds, and D. Kennedy, "The effect of air preheating in a biomass CFB gasifier using Aspen Plus simulation," *Biomass and Bioenergy*, vol. 33, no. 9, pp. 1158–1167, 2009.

[32] A. C. C. Chang, H.-F. Chang, F.-J. Lin, K.-H. Lin, and C.-H. Chen, "Biomass gasification for hydrogen production," *International Journal of Hydrogen Energy*, vol. 36, no. 21, pp. 14252–14260, 2011.

[33] A. Molino, V. Larocca, S. Chianese, and D. Musmarra, "Biofuels production by biomass gasification: a review," *Energies*, vol. 11, no. 4, p. 811, 2018.

[34] S. Safarian, C. Richter, and R. Unnthorsson, "Waste biomass gasification simulation using Aspen Plus: performance evaluation of wood chips, sawdust and mixed paper wastes," *Journal of Power and Energy Engineering*, vol. 7, no. 6, pp. 12–30, 2019.